Original Article | Pediatric Imaging

eISSN 2005-8330
https://doi.org/10.3348/kjr.2019.0824
Korean J Radiol 2020;21(12):1372-1378

Korean Journal of Radiology
KJR

Assessment of Diffusion Tensor Imaging Parameters of Hepatic Parenchyma for Differentiation of Biliary Atresia from Alagille Syndrome

Ahmed Abdel Khalek Abdel Razek, MD[1], Ahmed Abdalla, MD[2], Reda Elfar, MD[2], Germeen Albair Ashmalla, MD[1], Khadiga Ali, MD[3], Tarik Barakat, MD[2]

[1]Departments of Diagnostic Radiology and [3]Pathology, Mansoura Faculty of Medicine, Mansoura, Egypt; [2]Gastroenterology and Hepatology Unit, Mansoura Children Hospital, Mansoura Faculty of Medicine, Mansoura, Egypt

Objective: To assess diffusion tensor imaging (DTI) parameters of the hepatic parenchyma for the differentiation of biliary atresia (BA) from Alagille syndrome (ALGS).

Materials and Methods: This study included 32 infants with BA and 12 infants with ALGS groups who had undergone DTI. Fractional anisotropy (FA) and mean diffusivity (MD) of the liver were calculated twice by two separate readers and hepatic tissue was biopsied. Statistical analyses were performed to determine the mean values of the two groups. The optimum cut-off values for DTI differentiation of BA and ALGS were calculated by receiver operating characteristic (ROC) analysis.

Results: The mean hepatic MD of BA (1.56 ± 0.20 and 1.63 ± 0.2 x 10^{-3} mm^2/s) was significantly lower than that of ALGS (1.84 ± 0.04 and 1.79 ± 0.03 x 10^{-3} mm^2/s) for both readers (r = 0.8, p = 0.001). Hepatic MD values of 1.77 and 1.79 x 10^{-3} mm^2/s as a threshold for differentiating BA from ALGS showed accuracies of 82 and 79% and area under the curves (AUCs) of 0.90 and 0.91 for both readers, respectively. The mean hepatic FA of BA (0.34 ± 0.04 and 0.36 ± 0.04) was significantly higher (p = 0.01, 0.02) than that of ALGS (0.30 ± 0.06 and 0.31 ± 0.05) for both readers (r = 0.80, p = 0.001). FA values of 0.30 and 0.28 as a threshold for differentiating BA from ALGS showed accuracies of 75% and 82% and AUCs of 0.69 and 0.68 for both readers, respectively.

Conclusion: Hepatic DTI parameters are promising quantitative imaging parameters for the detection of hepatic parenchymal changes in BA and ALGS and may be an additional noninvasive imaging tool for the differentiation of BA from ALGS.

Keywords: *Diffusion tensor imaging; Biliary atresia; Jaundice; Infant*

INTRODUCTION

Biliary atresia (BA) is characterized by the luminal obstruction of the extrahepatic bile duct by a fibrous ductal remnant, which represents the obliterated ductal remnant in the porta hepatis at surgery. If infants with BA are left untreated, progressive liver cirrhosis leads to death by 2 years of age. Alagille syndrome (ALGS) is a genetic disease involving multiple organs with varying degrees of severity. The primary pathology of liver involvement is a paucity of intralobular bile ducts with subsequent chronic, progressive cholestasis (1-3). The most prevalent early clinical presentation of infants with ALGS is neonatal cholestatic jaundice. Differentiation between BA and AGS is difficult because of significant clinical, laboratory, radiological, and histopathological overlap leading to misdiagnosis. However, prompt discrimination of ALGS from BA is important as Kasai portoenterostomy is unlikely to be of value when the surgery is performed on infants older than 3 months of age with BA. Furthermore, Kasai portoenterostomy does not benefit infants with ALGS and may actually worsen their outcomes (3-5). Abnormal gallbladder shape, triangular cord sign, and hepatic artery enlargement are the main

Received: July 5, 2019 **Revised:** March 22, 2020
Accepted: April 18, 2020
Corresponding author: Ahmed Abdel Khalek Abdel Razek, MD, Department of Diagnostic Radiology, Mansoura Faculty of Medicine, Elgomheryia street, Mansoura 3512, Egypt.
• E-mail: arazek@mans.edu.eg

Korean Journal of Radiology
KJR

ultrasound discriminators of BA; however, the results are overlapping (6, 7). The assessment of extra-hepatic bile ducts can be done by magnetic resonance (MR) or intraoperative cholangiopancreatography (8, 9). Few studies have discussed the role of ultrasound in the differentiation of BA from ALGS because both present early with neonatal cholestasis (10, 11).

Diffusion-weighted imaging (DWI) exploits the translational Brownian motion of water protons by applying pairs of opposing magnetic field gradients. DWI has been used for the characterization of pediatric tumors, grading of hepatic fibrosis in infants and adults (12-16), and assessment of hepatic fibrosis in BA (14). Diffusion tensor imaging (DTI) is a recently introduced MR technique to assess tissue structure that provides insight into the micro-movements of water molecules and can be used to characterize different tissue compartments at the cellular level with different matrices. DTI utilizes additional gradients in various dimensions and has potential advantages for the estimation of fibrosis because different diffusion directions are calculated (17, 18). The parameters commonly used in DTI are fractional anisotropy (FA) and mean diffusivity (MD). The MD estimates the sum of the average diffusion properties of water molecules within each voxel to provide apparent diffusion coefficient (ADC) values over three orthogonal planes, assuming isotropy along each direction of movement. FA captures the directionality of diffusion and is considered an index for diffusion asymmetry within a voxel (18, 19). Different organs and tissues have different diffusion characteristics; among these, the liver has an anisotropic diffusion pattern due to its randomly organized structures, unlike the diffusion patterns of the kidney and brain (20). Several studies have verified the importance of DTI for assessing liver fibrosis using MD and FA (21-24) and have discussed the value of DTI in neonatal cholestasis using tailored and adapted DTI sequences for the differentiation of pediatric liver diseases (25-27). One study reported that hepatic MD can be used as an adjunct to other non-invasive imaging methods in the differential diagnosis of BA and non-BA, in which the MD showed a decreasing trend, whereas the FA showed an increasing trend with increasing fibrotic stage of BA (25). Another study added that DWI can be used for the evaluation of focal and diffuse liver diseases in pediatric patients using either mono-exponential, bi-exponential, or stretched DWI modules (27). In this study, we aimed to assess DTI parameters of hepatic parenchyma for the differentiation of BA from ALGS.

MATERIAL AND METHODS

Patients

This prospective study was approved by the Institutional Review Board (MS/16.12.29) and informed consent was obtained from the parents of the infants. This included infants with cholestatic jaundice who were referred to the radiology department between March 2013 and November 2018. The inclusion criteria were infants with cholestatic jaundice and unconjugated hyperbilirubinemia. The exclusion criteria were infants older than 3 months of age, unbiopsied cases, technically limited DTI examination of the liver, and diagnosis other than BA and ALGS. Technically limited DTI was reported in two patients due to infant motion artifacts during the MR examination. The final study group included 44 infants (30 girls, 14 boys, aged 24–90 days) with pathologically proven BA (n = 32) and ALGS (n = 12). Biochemical liver function tests were evaluated, including total and direct bilirubin and gamma-glutamyl transferase (γGT) levels.

MR Imaging

All MR images were acquired on a 1.5T superconducting body scanner (Ingenia, Philips Healthcare) using a 16-element phased-array surface coil (dStream Torso coil, Philips Healthcare) with a posterior body coil embedded in the table (dStream Total Spine coil, Philips Healthcare). The machine was equipped with a self-shielding high-performance gradient set (30 mTm maximum gradient strength). All patients were fasted for 4–6 hours before the study. Sedation was achieved using oral chloral hydrate (70–80 mg/kg body weight administered 30 minutes before the MR examination). Conventional MR of the upper abdomen was first performed with the following parameters: routine axial T1-weighted images (repetition time [TR]/echo time [TE] = 500/20 ms) and T2-weighted images (TR/TE = 6000/80 ms) were obtained. Free-breathing single-shot echo-planar imaging DTI of the liver using mono-exponential curve fitting of the diffusion module was performed using parallel imaging. We used three b-values (0, 400, and 800 s/mm^2). The diffusion gradients were applied in six directions (x, y, z, xy, yz, and xz) and the following sequence parameters were used: TR/TE = 3596/70 ms, matrix = 64 x 64, interpolated to 256 x 256, six slices = 7–8 mm, interslice gap = 0.8–2 mm, average number = 1, echo-planar imaging factor = 35, field of view = 22–25 cm, and total scan duration = 7–8 minutes.

https://doi.org/10.3348/kjr.2019.0824

Image Analysis

Image analysis was performed by two radiologists expert in hepato-biliary imaging for 25 and 15 years respectively who were blinded to the clinical presentation and final pathological results. The images were transferred to the workstation (extended MR Workspace 2.6.3.5, Philips Healthcare). All conventional MR images were first evaluated for the presence of abnormal signal intensity of the hepatic parenchyma. The images were then loaded to the DTI software workstation (View Forum 7.2.0.1 exported patient image data, Philips Healthcare). Overall DTI image quality for parenchyma structure discrimination, distortion, and motion artifacts was assessed. Co-registration of the DTI maps to T2-weighted images was done for accurate placement of the regions of interest. Three round regions of interest, each measuring 20 mm^2, were placed using an electronic cursor at both liver lobes to ensure measurement of the whole hepatic parenchyma. The selected regions of interest (ROIs) were small and carefully set in a homogeneous area of hepatic parenchyma to avoid the vascular and biliary structures and 1 cm from the lateral border of the liver (Fig. 1). Care was taken to place the ROIs of the left liver lobe below the level of the portal vein to avoid motion artifact resulting from cardiac motion. The ROIs were small owing to the tiny size of the neonates. The ROIs were placed on three consecutive slices to automatically calculate the FA and MD values. The final FA and MD values used for analysis were the mean values of the nine ROIs. The FA values ranged from 0 to 1, were 1 indicated those structures allowing diffusion only along a single direction, whereas structures allowing completely free or isotropic diffusion should result in an FA of 0.

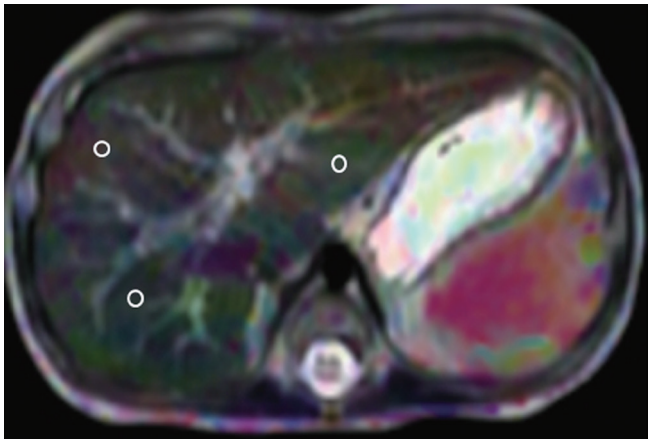

Fig. 1. Localization of ROIs. MD map showing localization of three ROIs within hepatic parenchyma. MD = mean diffusivity, ROIs = regions of interest

Pathology

All infants underwent ultrasound-guided Tru-Cut liver biopsy and the pathological specimens were evaluated by an expert pediatric pathologist. BA was diagnosed based on the presence of bile duct proliferation and bile plugs, while the diagnosis of hepatic involvement by ALGS was based on the paucity of intralobular biliary ducts (Fig. 2).

Statistical Analysis

The statistical analyses were performed using Statistical Package for Social Science version 10 (SPSS). The mean and standard deviation of the MD and FA values for BA and ALGS were calculated. Statistical differences were compared using either Fisher's exact test for categorical variables and two-sample *t*- or Mann-Whitney tests for continuous variables. Pearson correlations were used to estimate the proportion of inter-reader agreement for DTI parameters. Receiver operating characteristic (ROC) curves were generated to determine the cut-off points used to differentiate BA from ALGS. The sensitivity, specificity, accuracy, positive predictive value (PPV), negative predictive value (NPV), and the area under the curve (AUC) were calculated. Spearman correlation coefficient (*r*) was used to estimate the correlations between DTI parameters and pathological diagnoses. *P* values ≤ 0.05 were considered significant at a 95% confidence interval.

RESULTS

No statistical differences were observed in age and sex distributions between groups. Similarly, no significant differences in total and direct serum bilirubin and γGT levels were observed between infants with BA and those with ALGS (Table 1). No areas of abnormal signal intensity within the hepatic parenchyma were observed in either patient group.

Table 2 shows the MD and FA values for BA and ALGS determined by the two readers. Table 3 shows the results of the ROC curve analysis to determine the MD and FA cut-off values for BA and ALGS for the two readers.

The mean hepatic MD in infants with BA was 1.56 ± 0.20 and 1.63 ± 0.2 x 10^{-3} mm^2/s and in infants with ALGS was 1.84 ± 0.04 and 1.79 ± 0.03 x 10^{-3} mm^2/s for both readers, respectively, with significantly strong positive interreader correlation (r = 0.8, p = 0.001). The hepatic MD in infants with BA differed significantly from that of infants with ALGS (p = 0.001). MD values of 1.77 and 1.79 x 10^{-3} mm^2/s as

https://doi.org/10.3348/kjr.2019.0824

Korean Journal of Radiology
KJR

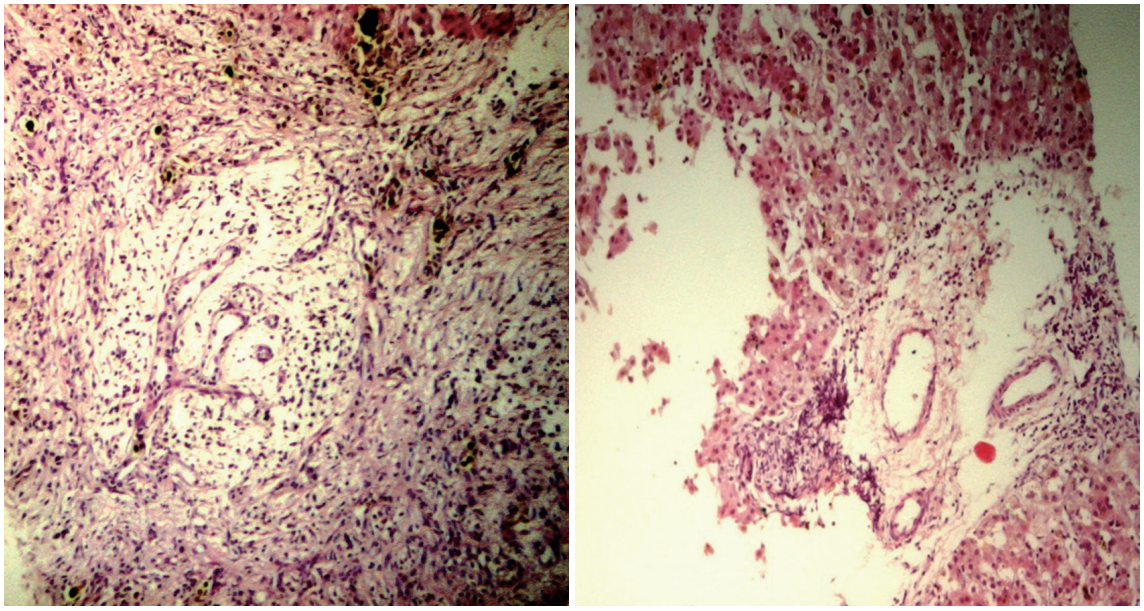

A B

Fig. 2. Liver biopsy of 2 infants with cholestasis.
A. Case of BA showing portal tract expansion by loose fibrous tissue containing irregularly anastomosing bile ductules at the periphery, some being dilated with inspissated bile in their lumen. **B.** Case of ALGS with portal area containing vessels but no ducts "unpaired artery" without cholangiolar proliferation (both are H & E stain, with magnification x 10). ALGS = Alagille syndrome, BA = biliary atresia

Table1. Demographic and Laboratory Results

	BA (n = 32)	ALGS (n = 12)	*P*
Age (months)	2.3 (1.0–11.0)	2.5 (1.0–24.0)	0.290
Total bilirubin (mg/dL)	13.7 ± 1.7	12.9 ± 2.4	0.180
Direct bilirubin (mg/dL)	7.3 ± 1.09	7.6 ± 1.1	0.420
γGT (IU/L)	521 ± 82.9	564 ± 88.5	0.140

Data are presented as mean (range values) or mean ± SD. ALGS = Alagille syndrome, BA = biliary atresia, γGT = gamma-glutamyl transferase

thresholds to differentiate BA from ALGS showed the best results, with accuracies of 82% and 79%, sensitivities of 91% and 83%, specificities of 80% and 78%, PPVs of 61% and 56%, NPVs of 96% and 93%, and AUCs of 0.90 and 0.91 for both readers, respectively (Fig. 3).

The mean hepatic FA in infants with BA was 0.34 ± 0.04 and 0.36 ± 0.04 and in infants with ALGS was 0.30 ± 0.06 and 0.31 ± 0.05 for both readers, respectively, showing a very strong positive correlation (r = 0.8, p = 0.001). The hepatic FA in infants with BA differed significantly from that of infants with ALGS (p = 0.001, 0.002 for both readers, respectively). An FA of 0.30 and 0.28 as a threshold value for differentiating BA from ALGS showed the best results, with accuracies of 75% and 82%, sensitivities of 81% and 93%, specificities of 58% and 50%, PPVs of 84% and 83%, NPVs of 54% and 75%, and AUCs of 0.69 and 0.68 for both readers, respectively (Fig. 4).

Table 2. MD and FA of Both Readings for BA and ALGS

DTI	BA (n = 32)	ALGS (n = 12)	*P*
MD (x 10^{-3} mm^2/s)			
1st reading	1.56 ± 0.20 (1.23–1.95)	1.84 ± 0.04 (1.82–1.97)	0.001
2nd reading	1.63 ± 0.20 (1.19–1.87)	1.79 ± 0.03 (1.73–1.86)	0.001
FA			
1st reading	0.34 ± 0.04 (0.22–0.40)	0.30 ± 0.06 (0.24–0.37)	0.001
2nd reading	0.36 ± 0.04 (0.24–0.40)	0.31 ± 0.05 (0.24–0.38)	0.002

Data are presented as mean ± SD (minimum–maximum values). DTI = diffusion tensor imaging, FA = fractional anisotropy, MD = mean diffusivity

A significant moderate positive correlation was observed between hepatic DTI parameters for both readers and pathological diagnosis (r = 0.376, p = 0.002 for the first reader and r = 0.357, p = 0.003 for the second reader).

DISCUSSION

The main finding in this study was that DTI parameters could quantitate early microstructural changes in the hepatic parenchyma of infants with BA and ALGS. The DTI parameters showed significantly lower hepatic MD

https://doi.org/10.3348/kjr.2019.0824

Table 3. ROC Curve Results of MD and FA of Both Readings for Differentiating BA and ALGS

	AUC	Cut-Off Point	Sensitivity (%)	Specificity (%)	PPV (%)	NPV (%)	Accuracy (%)
MD (x 10^{-3} mm^2/s)							
1st reading	0.90	1.77	91	80	61	96	82
2nd reading	0.91	1.79	83	78	56	93	79
FA							
1st reading	0.69	0.30	81	58	84	54	75
2nd reading	0.68	0.28	93	50	83	75	82

AUC = area under the curve, NPV = negative predictive value, PPV = positive predictive value, ROC = receiver operating characteristic

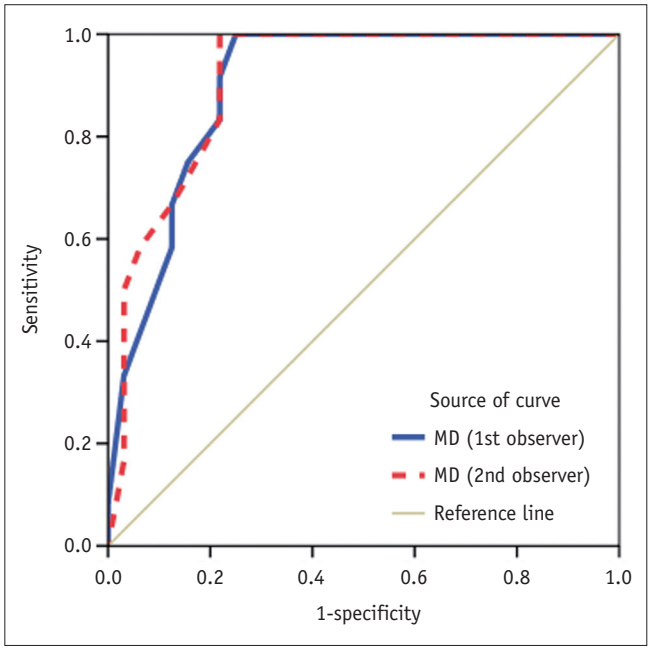

Fig. 3. ROC of MD used to differentiate BA from ALGS. MD of 1.77 and 1.79 x 10^{-3} mm^2/s as threshold value for differentiating BA from ALGS shows accuracies of 82% and 79%, sensitivities of 91% and 83%, specificities of 80% and 83%, and AUCs of 0.90 and 0.91 for both reviewers, respectively. AUC = area under the curve, ROC = receiver operating characteristic

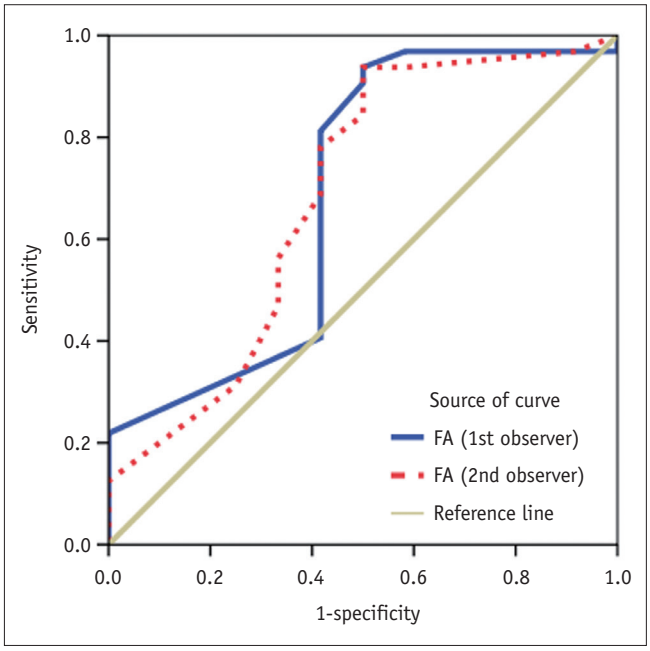

Fig. 4. ROC of FA used to differentiate BA from ALGS. FA of 0.30, 0.28 as threshold value for differentiating BA from ALGS shows accuracies of 79% and 82%, sensitivities of 81% and 93%, specificities of 58% and 50%, and AUCs of 0.69 and 0.68 for both readers, respectively. FA = fractional anisotropy

and significantly higher FA in infants with BA than those in patients with ALGS. A significant strong positive correlation was observed between the FA and MD for both readers. The DTI parameters of hepatic parenchymal show a significant moderate correlation with pathological diagnosis of BA and ALGS.

The clinical relevance of adding DTI to the workup of infants with neonatal cholestasis is the considerable overlap in clinical, laboratory, imaging, and pathological findings between infants with BA and those with ALGS. Ultrasound findings cannot differentiate between entities as these conditions may overlap in their pathological features including the paucity of interlobular bile ducts. This paucity is not always present in liver biopsy and the typical clinical features are not obviously present in all patients.

In this study, the hepatic MD of infants with BA was lower than that in those with ALGS while the hepatic FA in infants with BA was significantly higher than that in infants with ALGS. These findings can be explained in view of the underlying pathological process in these disease entities. Infants with BA showed destructive interlobular ducts, ductular proliferation, cellular biliary stasis, bile plugs, ductal plate malformation, inflammatory cell infiltration surrounding the proliferated bile ducts, porto-portal bridging hepatic fibrosis, and increased collagen production (1, 2), which are associated with restricted diffusion and subsequent reduction in MD (24-26) and disturbance of the normal isotropic diffusion within the liver parenchyma as well as increased anisotropy. ALGS is characterized by a non-destructive paucity or even absence of intralobular bile ducts (3, 4) due to a developmental defect in the ductal

https://doi.org/10.3348/kjr.2019.0824

Korean Journal of Radiology
KJR

plate and absence of the inflammatory response, which are associated with unrestricted diffusion and higher MD with more isotropic diffusion of the water molecules.

A previous study reported restricted diffusion in BA with lower hepatic MD compared to those in controls and that the diffusion change of the liver parenchyma in biliary cirrhosis was similar to those related to cirrhosis in chronic hepatitis (14). Another study evaluated the diagnostic performance of bi-exponential and stretched exponential modules with ten b values in infants with neonatal cholestasis, reported lower ADC 10, ADC 2, fast diffusion, perfusion fraction, and distribution diffusion coefficient and higher γGT and diffusion heterogeneity index in infants with BA compared to those without BA, with the best results obtained from ADC 2 using two b values (25). Another study observed higher diagnostic performance for the stretched exponential model for determining significant hepatic fibrosis compared to for the mono-exponential model (26).

The current study observed a significant difference in FA, which could be explained by the early investigation of the liver in BA before the development of fibrosis, in which collagen is deposited within the liver parenchyma, helping in the return of isotropic diffusion in the water molecules. The FA predominantly represents the degree of the directionality of water diffusion in the microstructure of the tissue, which is related to the orientation of different tissues (20-23). However, a previous study on neonatal cholestasis did not observe a difference in hepatic FA between BA and non-BA (24). This difference in findings may be attributed to differences in patient ages, protocols, and machines and parameters.

This technique is clinically reliable and robust, as we adopted the sequence for infants by using free-breathing with a low acquisition matrix and parallel imaging to eliminate repository motion effects. Moreover, we used localization based on nine ROIs to obtain diffusion data from both liver lobes. Previous studies reported that the breath-hold technique was not possible in neonates and that the respiratory triggering technique was less reproducible than free breathing with lengthy scan time (24). Previous studies used ROIs on DTI that were generally placed on the right hepatic lobe, with an effort to avoid interference from the surrounding abdominal wall, vascular and biliary structures, and cardiac cycle (25, 26). Additional studies are needed to compare DTI parameters obtained from both liver lobes and the right lobe only.

This study has several limitations. First, the small number of infants limited statistical analysis. Multicenter studies including a large number of patients are required. Second, there was a bias from the selection of ROI, texture analysis, and machine learning of DTI parameters, which may have affected the results. Third, this study used DTI on 1.5T scanners; further multiparametric study using DTI on higher-powered scanners combined with contrast, MR imaging, and proton MR spectroscopy will improve the results (28). Fourth, we did not include neonatal hepatitis, although it is one of the two most common causes of neonatal jaundice because they may be suspected clinically, Additional multicenter studies including all groups of infants with neonatal cholestasis are needed to evaluate role of DTI in the management of these patients.

In conclusion, hepatic DTI parameters are promising quantitative imaging parameters for the detection of hepatic parenchymal changes in BA and ALGS and may be an additional noninvasive imaging tool for the differentiation of BA from ALGS.

Conflicts of Interest

The authors have no potential conflicts of interest to disclose.

ORCID iDs

Ahmed Abdel Khalek Abdel Razek
https://orcid.org/0000-0002-9613-5932
Ahmed Abdalla
https://orcid.org/0000-0002-5829-123X
Reda Elfar
https://orcid.org/0000-0002-1416-2161
Germeen Albair Ashmalla
https://orcid.org/0000-0002-1085-7126
Khadiga Ali
https://orcid.org/0000-0001-7556-7173
Tarik Barakat
https://orcid.org/0000-0002-9423-4128

REFERENCES

1. Bezerra JA, Wells RG, Mack CL, Karpen SJ, Hoofnagle JH, Doo E, et al. Biliary atresia: clinical and research challenges for the twenty-first century. *Hepatology* 2018;68:1163-1173
2. Neto B, Borges-Dias M, Trindade E, Estevão-Costa J, Campos JM. Biliary atresia-clinical series. *GE Port J Gastroenterol* 2018;25:68-73
3. Mitchell E, Gilbert M, Loomes KM. Alagille syndrome. *Clin Liver Dis* 2018;22:625-641

 https://doi.org/10.3348/kjr.2019.0824

4. Kamath BM, Baker A, Houwen R, Todorova L, Kerkar N. Systematic review: the epidemiology, natural history, and burden of Alagille syndrome. *J Pediatr Gastroenterol Nutr* 2018;67:148-156
5. Emerick KM, Rand EB, Goldmuntz E, Krantz ID, Spinner NB, Piccoli DA. Features of Alagille syndrome in 92 patients: frequency and relation to prognosis. *Hepatology* 1999;29:822-829
6. Lee SM, Cheon JE, Choi YH, Kim WS, Cho HH, Kim IO, et al. Ultrasonographic diagnosis of biliary atresia based on a decision-making tree model. *Korean J Radiol* 2015;16:1364-1372
7. Hwang SM, Jeon TY, Yoo SY, Choe YH, Lee SK, Kim JH. Early US findings of biliary atresia in infants younger than 30 days. *Eur Radiol* 2018;28:1771-1777
8. Lin DC, Wu KY, Sun FJ, Huang CC, Wu TH, Shih SL, et al. A quantitative image analysis using MRI for diagnosis of biliary atresia. *Clin Imaging* 2019;53:186-190
9. Kim YH, Kim MJ, Shin HJ, Yoon H, Han SJ, Koh H, et al. MRI-based decision tree model for diagnosis of biliary atresia. *Eur Radiol* 2018;28:3422-3431
10. Han S, Jeon TY, Hwang SM, Yoo SY, Choe YH, Lee SK, et al. Imaging findings of Alagille syndrome in young infants: differentiation from biliary atresia. *Br J Radiol* 2017;90:20170406
11. Cho HH, Kim WS, Choi YH, Cheon JE, Lee SM, Kim IO, et al. Ultrasonography evaluation of infants with Alagille syndrome: in comparison with biliary atresia and neonatal hepatitis. *Eur J Radiol* 2016;85:1045-1052
12. Razek AAKA, Abdalla A, Barakat T, El-Taher H, Ali K. Assessment of the liver and spleen in children with Gaucher disease type I with diffusion-weighted MR imaging. *Blood Cells Mol Dis* 2018;68:139-142
13. Razek AA, Massoud SM, Azziz MR, El-Bendary MM, Zalata K, Motawea EM. Prediction of esophageal varices in cirrhotic patients with apparent diffusion coefficient of the spleen. *Abdom Imaging* 2015;40:1465-1469
14. Mo YH, Jaw FS, Ho MC, Wang YC, Peng SS. Hepatic ADC value correlates with cirrhotic severity of patients with biliary atresia. *Eur J Radiol* 2011;80:e253-e257
15. Razek AAKA, Khashaba M, Abdalla A, Bayomy M, Barakat T. Apparent diffusion coefficient value of hepatic fibrosis and inflammation in children with chronic hepatitis. *Radiol Med* 2014;119:903-909
16. Razek AA, Abdalla A, Omran E, Fathy A, Zalata K. Diagnosis and quantification of hepatic fibrosis in children with diffusion weighted MR imaging. *Eur J Radiol* 2011;78:129-134
17. Razek AAKA, Al-Adlany MAAA, Alhadidy AM, Atwa MA, Abdou NEA. Diffusion tensor imaging of the renal cortex in diabetic patients: correlation with urinary and serum biomarkers. *Abdom Radiol (NY)* 2017;42:1493-1500
18. Abdel Razek AAK. Routine and advanced diffusion imaging modules of the salivary glands. *Neuroimaging Clin N Am* 2018;28:245-254
19. El-Serougy L, Abdel Razek AA, Ezzat A, Eldawoody H, El-Morsy A. Assessment of diffusion tensor imaging metrics in differentiating low-grade from high-grade gliomas. *Neuroradiol J* 2016;29:400-407
20. Taouli B, Vilgrain V, Dumont E, Daire JL, Fan B, Menu Y. Evaluation of liver diffusion isotropy and characterization of focal hepatic lesions with two single-shot echo-planar MR imaging sequences: prospective study in 66 patients. *Radiology* 2003;226:71-78
21. Cheung JS, Fan SJ, Gao DS, Chow AM, Man K, Wu EX. Diffusion tensor imaging of liver fibrosis in an experimental model. *J Magn Reson Imaging* 2010;32:1141-1148
22. Tosun M, Inan N, Sarisoy HT, Akansel G, Gumustas S, Gürbüz Y, et al. Diagnostic performance of conventional diffusion weighted imaging and diffusion tensor imaging for the liver fibrosis and inflammation. *Eur J Radiol* 2013;82:203-207
23. Taouli B, Chouli M, Martin AJ, Qayyum A, Coakley FV, Vilgrain V. Chronic hepatitis: role of diffusion-weighted imaging and diffusion tensor imaging for the diagnosis of liver fibrosis and inflammation. *J Magn Reson Imaging* 2008;28:89-95
24. Kwee TC, Takahara T, Koh DM, Nievelstein RA, Luijten PR. Comparison and reproducibility of ADC measurements in breathhold, respiratory triggered, and free-breathing diffusion-weighted MR imaging of the liver. *J Magn Reson Imaging* 2008;28:1141-1148
25. Liu B, Cai J, Zhu J, Zheng H, Zhang Y, Wang L. Diffusion tensor imaging for evaluating biliary atresia in infants and neonates. *PLoS One* 2016;11:e0168477
26. Kim J, Yoon H, Lee MJ, Kim MJ, Han K, Han SJ, et al. Clinical utility of mono-exponential model diffusion weighted imaging using two b-values compared to the bi- or stretched exponential model for the diagnosis of biliary atresia in infant liver MRI. *PLoS One* 2019;14:e0226627
27. Yoon H, Shin HJ, Kim MJ, Lee MJ. Quantitative imaging in pediatric hepatobiliary disease. *Korean J Radiol* 2019;20:1342-1357
28. Razek AA, Nada N. Correlation of choline/creatine and apparent diffusion coefficient values with the prognostic parameters of head and neck squamous cell carcinoma. *NMR Biomed* 2016;29:483-489

https://doi.org/10.3348/kjr.2019.0824